

Article

# Atmospheric Pressure Plasma Surface Treatment of Rayon Flock Synthetic Leather with Tetramethylsilane

Chi-Wai Kan <sup>1,\*</sup>, Chi-Ho Kwong <sup>1</sup> and Sun-Pui Ng <sup>2</sup>

<sup>1</sup> Institute of Textiles and Clothing, Hong Kong Polytechnic University, Hung Hom, Kowloon, Hong Kong 00852, China; chris.kwong@connect.polyu.hk

<sup>2</sup> Hong Kong Community College, Hong Kong Polytechnic University, Hung Hom, Kowloon, Hong Kong 00852, China; ccspng@hkcc-polyu.edu.hk

\* Correspondence: tccwk@polyu.edu.hk; Tel.: +852-2766-6531; Fax: +852-2773-1432

Academic Editor: Samuel Adeloju

Received: 11 December 2015; Accepted: 4 February 2016; Published: 22 February 2016

**Abstract:** This paper investigates the use of atmospheric pressure plasma (APP) treatment for improving the surface hydrophobicity of rayon flock synthetic leather with organosilane precursor (tetramethylsilane (TMS)). Plasma deposition of TMS is regarded as an effective, simple, and low-pollution process. The results show that a highly hydrophobic surface is formulated on the rayon flock synthetic leather. Under a particular combination of treatment parameters, a hydrophobic surface was achieved on the APP-treated sample with a contact angle of 135° while the untreated sample had a contact angle of 0° (*i.e.*, the fabric surface was completely drenched immediately). Scanning Electron Microscopy (SEM), Fourier Transform Infrared Spectroscopy (FTIR), and X-ray Photoelectron Spectroscopy (XPS) confirmed the deposition of organosilane.

**Keywords:** atmospheric pressure plasma; hydrophobic; rayon flock; synthetic leather; contact

## 1. Introduction

Rayon flock is a synthetic leather having a flexible backing and multiple upstanding flock fibers adhered to the backing. It has a layer of rayon flocking hair held by adhesive on a rayon cloth. It is usually used as upholstery for sofas and automobiles. Owing to the hydrophilic nature of rayon (regenerated cellulosic fiber), it can be easily stained. This problem can be alleviated by improving surface hydrophobicity. Many researchers have explored ways of improving the flock surface hydrophobicity. Shang *et al.* prepared a transparent, superhydrophobic, silica-based surface film by introducing a nano-scale rough surface [1]. Huang *et al.* confirmed that a superhydrophobic surface can be achieved by aligned carbon nanotubes coated with a thin zinc oxide film [2]. Lee and Michielson enhanced the surface hydrophobicity of nylon flock fabric by grafting with poly(acrylic acid) and 1H-1H-perfluorooctyl-amine [3]. Kim *et al.* fabricated a hydrophobic coating by CF<sub>4</sub> plasma treatment [4].

Among the different methods, plasma treatment of a polymer surface is an effective technique because of its unique ability to form a thin hydrophobic film on surfaces [5]; this technique can be integrated into continuous production processes [6] also, which means a single-step method for surface modification. Plasma treatment of polymer surface is a well-established technique [7–9]. Atmospheric pressure plasma overcomes the disadvantages of low-pressure plasma—its integration into an in-line production process is cumbersome and expensive [10]. Traditional plasma sources include transferred arcs, corona discharge, and dielectric barrier discharge (DBD) [10]. Corona and DBD produced non-equilibrium plasmas, with gas temperature between 50 °C and 400 °C, which may limit their usage in materials processing [10]. On the other hand, atmospheric pressure plasma

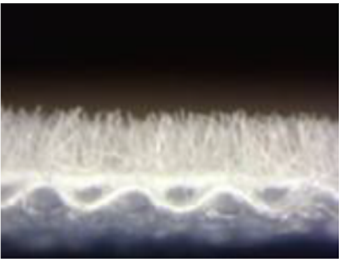
offers the advantages of a temperature range from 20 °C to 200 °C with a high concentration of reactive species from 10 ppm to 100 ppm [10]. Atmospheric pressure plasma jet is an effective way to create a plasma zone with its movable torch [11]. A number of researchers have studied the possible applications of the plasma torch [11,12]. It could be a single-step method for surface hydrophobization. Because of its stability and low toxicity, organosilane is one of the monomers for introducing a hydrophobic surface [12–15]. In previous studies [16–19], tetramethylsilane (TMS) has been applied to modify a synthetic leather surface under the influence of atmospheric pressure plasma treatment. The hydrophobicity of a TMS-plasma-treated synthetic leather surface, which is a flat surface, was improved significantly. However, TMS plasma treatment for synthetic leather with a flock surface has seldom been reported. Therefore, in this study, the surface of rayon flock synthetic leather is modified by means of atmospheric pressure plasma using a plasma jet with TMS and the chemical and morphological changes on the surface are evaluated by instrumental methods. In addition, the statistical method SPSS is used for finding the correlation between the treatment parameters.

## 2. Experimental Section

### 2.1. Materials

Rayon flock synthetic leather was supplied by Fifield Ltd (Hong Kong, China). The synthetic leather was cut into sample pieces of 1 cm × 2.5 cm for APP treatment. The samples were stored in a conditioning room at 65% ± 2% relative humidity and 21 ± 1 °C temperature for 24 h prior to the experiment. The basic information of the synthetic leather is listed in the Table 1.

**Table 1.** Basic information of rayon flock synthetic leather [20].

Composition	Picture
Flocking facing with woven backing (100% rayon flock, 100% rayon woven backing)	

### 2.2. Atmospheric Pressure Plasma (APP) Treatment

An atmospheric pressure plasma generator, Atomflo™ 200 (Surfx Technology, Redondo Beach, CA, USA) was used for the APP treatment. Gas discharge was generated by applying a radio frequency of 13.56 MHz. The APP jet was placed vertically over the sample in the experiment. Figure 1 shows the experimental setup for APP treatment. Helium was used as the carrier gas and tetramethylsilane (TMS) (ACROS, 99%) was applied as a precursor. Various combinations of treatment parameters, discharge power (30 W, 40 W, 50 W, and 60 W), flow rate of helium (7.5 L per minute (LPM), 10.0 LPM, 12.5 LPM, 15.0 LPM, and 17.5 LPM), amount of TMS (per L of helium) (0 mL, 0.1 mL, 0.15 mL, 0.2 mL and 0.25 mL), treatment time (10 s, 20 s, 30 s, and 40 s), and jet distance (10 mm) were used for making the surface hydrophobic. After plasma treatment, the samples were stored in a conditioning room at 65% ± 2% relative humidity and 21 ± 1 °C for 24 h before further experiment.

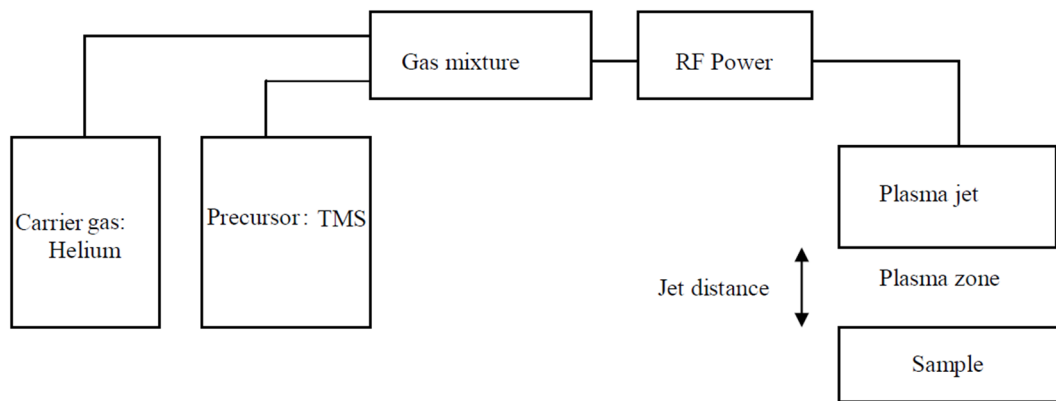


**Figure 1.** Schematic diagram of APP treatment.

### 2.3. Contact Angle and Surface Energy

The surface hydrophobicity was quantified by measurement of the contact angle with a goniometer [21]. A drop of 5  $\mu\text{L}$  deionized water was used to probe the sample surface. The droplet images were recorded with a high-resolution camera. The contact angle was precisely measured in the picture. Five readings were taken from each sample and the mean was calculated. The measurement was done immediately after APP treatment. The surface energy of the plasma-modified samples was determined using the Kaelble’s two-liquids method, as given in Equation (1) and (2) [22]. Two probing liquids, deionized water (72.8 mN/m) and glycerol (63.4 mN/m), were used for contact angle measurement according to the standard testing method ASTM D5946. Table 2 shows the discrete values of dispersion ( $\gamma_1^d$ ) and polar ( $\gamma_1^p$ ) parts of the surface tension ( $\gamma_1$ ) used for calculation [22].

**Table 2.** Dispersion and polar contributions to liquid surface tension.

Liquid	$\gamma_1$	$\gamma_1^d$	$\gamma_1^p$
Water	72.8	21.8	51.0
Glycerol	63.4	37.0	26.4

$$\gamma_l(1 + \cos\theta) = 2 \times [(\gamma_{sp} \times \gamma_{lp})^{1/2} + (\gamma_{sd} \times \gamma_{ld})^{1/2}] \tag{1}$$

$$\gamma_s = \gamma_{sp} + \gamma_{sd} \tag{2}$$

where:  $\theta$  is the static contact angle between the rayon flock synthetic leather and the probing liquid;  $\gamma_l$  is the surface tension of the probing liquid;  $\gamma_1^p$  and  $\gamma_1^d$  are the polar and dispersive components, respectively, of the probing liquid;  $\gamma_s$  is the overall surface energy of the rayon flock synthetic leather; and  $\gamma_s^p$  and  $\gamma_s^d$  are the polar and dispersive components, respectively, of the rayon flock synthetic leather.

### 2.4. Sliding Angle Measurement

The hydrophobic behavior of the plasma-treated samples was also measured by its sliding angle by mounting it on an acrylic plastic plate, as shown in Figure 2. During the measurement, a drop of 5  $\mu\text{L}$  deionized water was probed on the sample surface and the plastic plate was then tilted until the water droplet started to slide. The tilting angle,  $\alpha$  (termed as sliding angle), is the angle at which the water droplet starts to slide. The lower the sliding angle, the slicker the surface is. The slicker the surface, the less water can stick and hence better hydrophobicity.

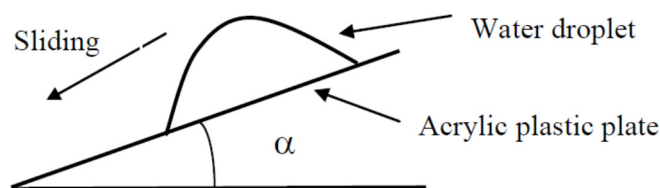


**Figure 2.** Sliding angle measurement.

### 2.5. Scanning Electron Microscopy (SEM)

JEOL Model JSM-6490 SEM was used for observation of the surface morphological changes. Before SEM analysis, the samples were coated with gold by a sputter coater (SCD005, BAL-TEC, Balzers, Liechtenstein) under vacuum state. Silver paint was used to connect the sample and disc holder to ensure the sample was electrically conductive. The magnification of the image ranged from  $3000\times$  to  $5000\times$ , captured with 20 kV accelerating voltage for investigating the surface.

### 2.6. Fourier Transform Infrared Spectroscopy (FTIR-ATR)

Perkin Elmer spectrophotometer (Spectrum 100, Perkin Elmer Ltd., Waltham, MA, USA) equipped with an attenuated total internal reflectance (ATR) accessory was used to analyze the chemical functionalities of the samples. Each FTIR spectrum was obtained after an average of 64 scans with a resolution of  $4\text{ cm}^{-1}$ .

### 2.7. X-Ray Photoelectron Spectroscopy (XPS)

XPS analysis was carried out with an SKL-12 spectrometer (Leybold Heraeus, Shengyang, China) modified with VG CLAM 4 multi-channel hemispherical analysis equipped with Al/Mg twin anode. The spectrometer was operated with non-monochromatic Mg  $K\alpha$  (1253.6 eV) radiation for the characterization of the plasma-modified substrate under vacuum condition of  $8 \times 10^{-8}$  Pa. To compensate for surface charging effects, all binding energies were referenced to the C1s peak at 285.0 eV. Spectra were analyzed and curve fitting was done with the aid of XPSpeak 4.1. (Informer Technologies Inc, Hong Kong, China, 2000) Moreover, the content of each chemical component with C1s are calculated by deconvolution analysis. Four distinct sub-peaks corresponding to C–H or C–C (285.0 eV), C–O (286.9 eV), C=O (288.0 eV), and O–C–O (288.7 eV) were observed.

### 2.8. Multiple Linear Regression Model

SPSS 14.0 (SPSS Ltd., Hong Kong, China, 2006) was used for developing the regression model, which is able to find the correlation between dependent and independent parameters.

## 3. Results and Discussion

### 3.1. Effects of Discharge Power and Flow Rate of Helium

Without the plasma treatment, the contact angle of the rayon flock synthetic leather is  $0^\circ$ . Figure 3 shows the contact angles of rayon flock synthetic leather after TMS plasma treatment. The results show that the contact angle can be decreased with an increase in the helium flow rate. Remarkable enhancement in contact angle was observed under all discharge powers. At a discharge power of 30 W, the contact angle fluctuates with respect to the flow rates of helium. The fluctuation is attributed to insufficient discharge power. The ionization of TMS is unstable without sufficient energy provided from discharge power. A discharge power of 50 W results in stability and the best improvement in contact angle (helium flow rate of 12.5 LPM). Further increase in power did not promote enhancement in contact angle. The ionization of the TMS might have occurred at a discharge power of around 50 W. It is suggested that adequate power is required for plasma deposition.

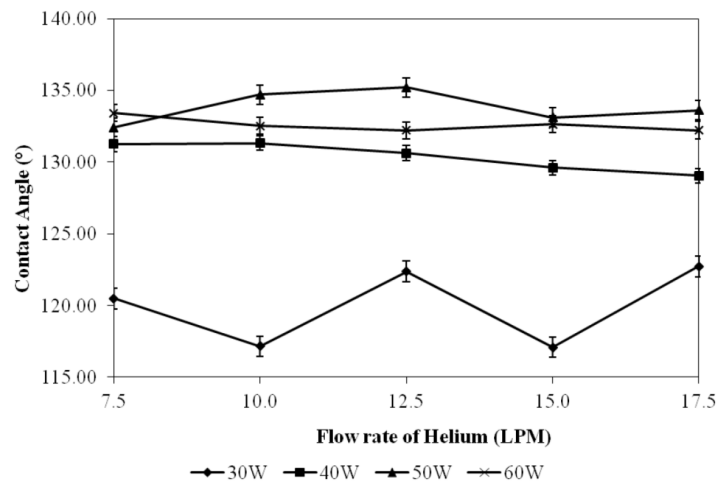


**Figure 3.** Contact angle of rayon flock synthetic leather after TMS plasma treatment (treatment parameters: amount of TMS = 0.2 mL; jet distance = 10 mm; treatment time = 30 s).

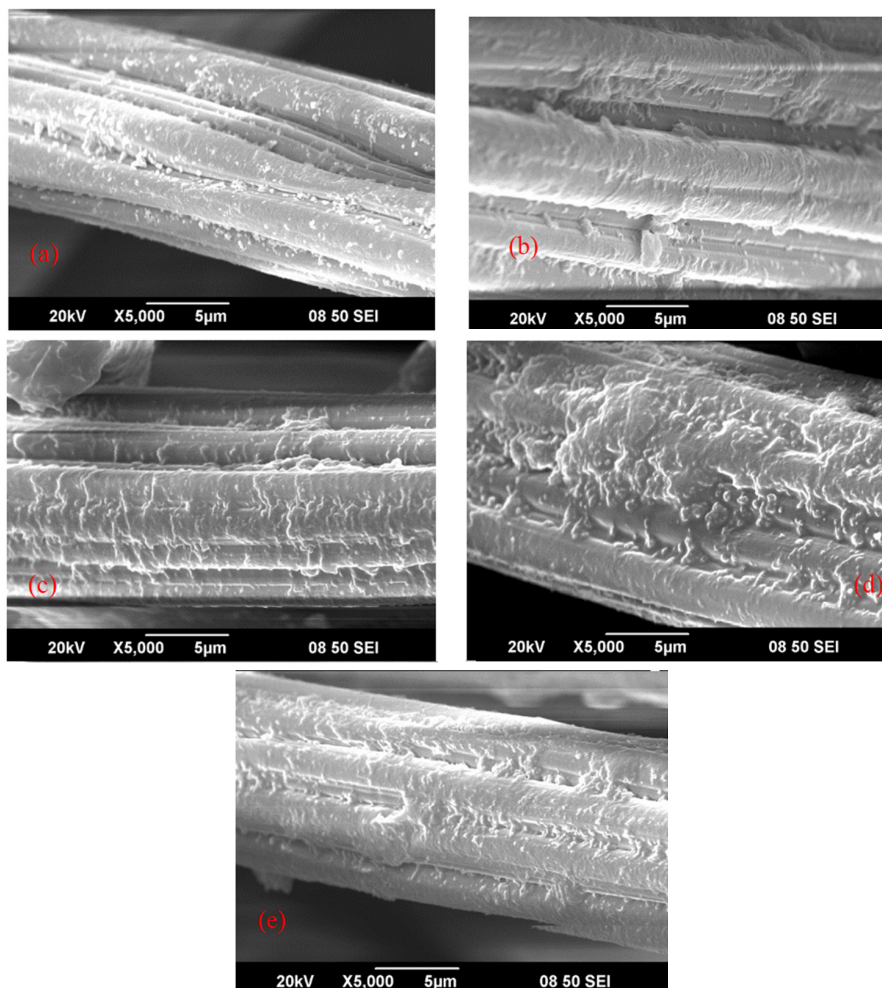


**Figure 4.** SEM micrographs illustrate the surface morphology of rayon flock synthetic leather after TMS plasma treatment with different discharge power: (a) untreated, (b) 30 W, (c) 40 W, (d) 50 W, (e) 60 W (treatment parameters: amount of TMS = 0.2 mL; flow rate of helium = 12.5 LPM; jet distance = 10 mm; treatment time = 30 s).

The surface morphology of rayon flock synthetic leather modified with different discharge power was examined by SEMs (Figure 4). The untreated sample surface (Figure 4a) is relatively smooth while nubs and burrs appear on the surface of the plasma modified samples [22]. A small number of nubs and burrs are deposited on the sample surface with a discharge power of 30 W, as shown in Figure 4b. The number of nubs and burrs on the plasma-modified samples increase when the power is increased from 30 W to 50 W (Figure 4b–d). However, the number of nubs and burrs drops at a discharge power of 60 W (Figure 4e). The SEM images indicate that a discharge power of 50 W (Figure 4d) promotes the deposition of silicon compounds from TMS effectively, irrespective of the discharge power.

### 3.2. Effect of Treatment Time

Figure 5 illustrates the surface morphology of rayon flock synthetic leather after TMS plasma treatment with different treatment times. Figure 5a shows that a sample with a treatment time of 10 s has a relatively smooth surface. A small number of nubs and burrs are deposited on it. The number of nubs and burrs on the plasma-modified samples increases with treatment time, as shown in Figure 5b,c. However, after the treatment time exceeds 30 s (Figure 5d), there is no further increase in deposition.

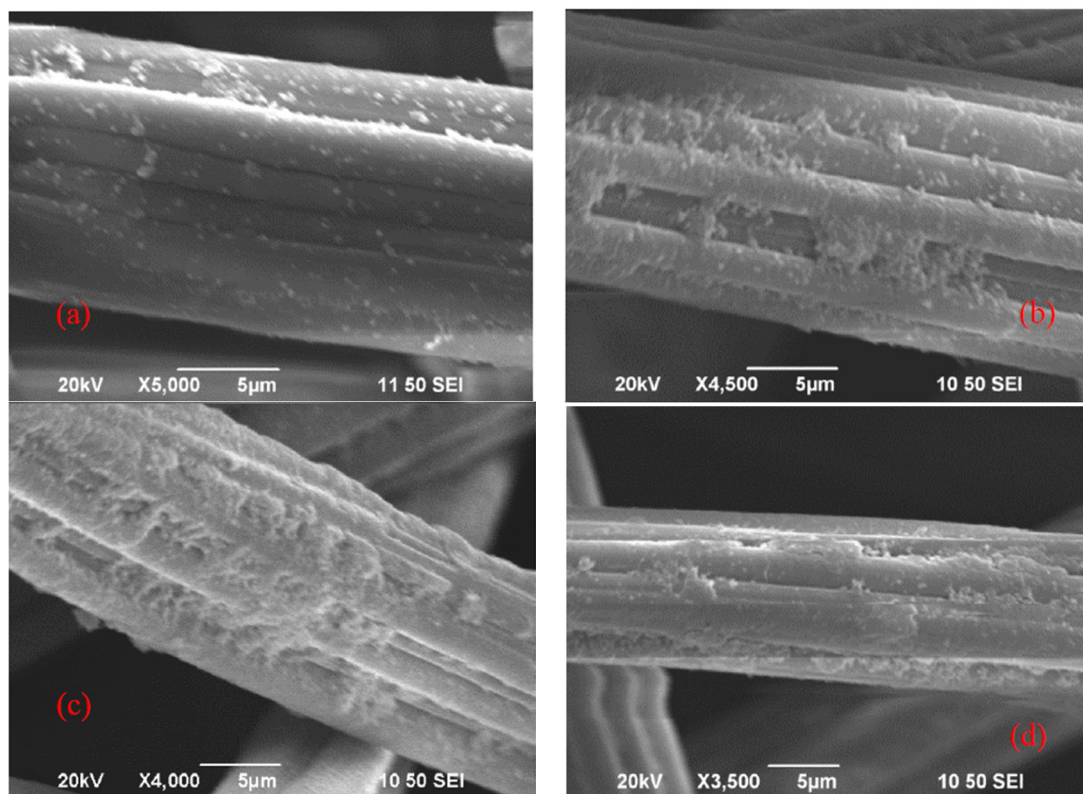


**Figure 5.** SEM micrographs illustrate the surface morphology of rayon flock synthetic leather after TMS plasma treatment with different treatment times: (a) 10 s, (b) 20 s, (c) 30 s, (d) 40 s (treatment parameters: amount of TMS = 0.2 mL; flow rate of helium = 12.5 LPM; jet distance = 10 mm; discharge power = 50 W).

### 3.3. Effect of Amount of TMS

Figure 6 illustrates the surface morphology of rayon flock synthetic leather after TMS plasma treatment with different amounts of TMS. Figure 6a shows that sample with 0.1 mL TMS has a relatively smooth surface and a small number of nubs and burrs are deposited on it. The TMS deposited is insufficient for surface hydrophobicity improvement. The number of nubs and burrs on the plasma

modified samples increases with amount of TMS applied, as shown in Figure 6b,c. After reaching the optimum amount of 0.2 mL TMS (Figure 6c), there is no further increase in deposition (Figure 6d).

Table 3 shows the change of contact angle of rayon flock synthetic leather treated with different amount of TMS under the effect of plasma. It is noted that without the addition of TMS, no change in contact angle is seen when compared with the untreated sample. However, with an increasing amount of TMS, the contact angle increases, with an optimum at 0.2 mL. Further increase in TMS to 0.25 mL does not introduce further enhancement in the contact angle. When compared with Figure 6c,d, the deposition of TMS under the plasma treatment reaches a maximum at 0.2 mL TMS. Therefore, the contact angle results are supported by the surface morphological changes, with an increased amount of TMS deposited in the rayon flock synthetic leather surface.

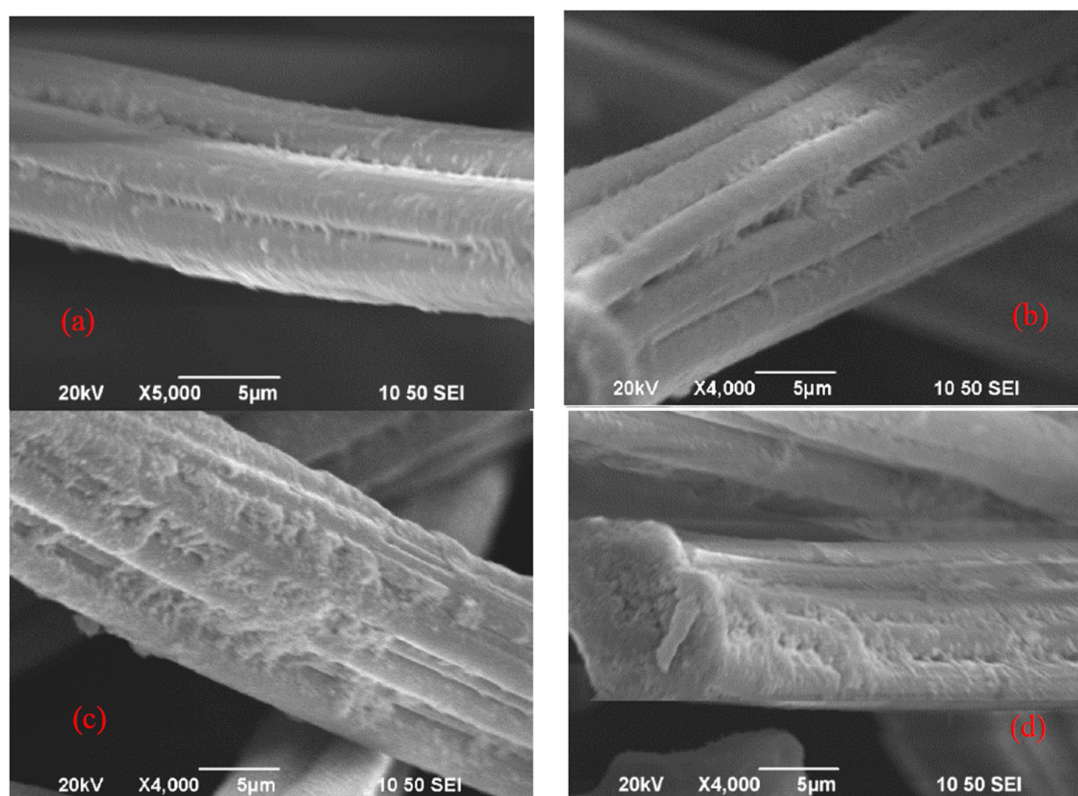


**Figure 6.** SEM micrographs illustrate the surface morphology of rayon flock leather after TMS plasma treatment with different amounts of TMS: (a) 0.1 mL, (b) 0.15 mL, (c) 0.2 mL, (d) 0.25 mL (treatment parameters: treatment time = 30 s; flow rate of helium = 12.5 LPM; jet distance = 10 mm; discharge power = 50 W).

**Table 3.** Effect of amount of TMS on contact angle (treatment parameters: treatment time = 30 s; flow rate of helium = 12.5 LPM; jet distance = 10 mm; discharge power = 50 W) ( $n = 5$ ).

Amount of TMS (mL)	Untreated	0 (Treated With Helium Plasma Only)	0.1	0.15	0.2	0.25
Contact angle (°)	0	0	47.4 ± 0.1	74.9 ± 0.2	135 ± 0.1	102.2 ± 0.2
Sliding angle (°)	0	0	72 ± 0.2	56 ± 0.2	32 ± 0.2	45 ± 0.3

In order to have a better understanding of the surface hydrophobicity of rayon flock synthetic leather, the change in the sliding angle of rayon flock synthetic leather treated with different amounts of TMS under the effect of plasma is reported in Table 3. Generally speaking, the lower the sliding angle, the slicker the surface is. The slicker the surface, the less things like water and contaminants can stick and hence the better the hydrophobicity. As shown in Table 3, the sliding angle decreases with an

increasing amount of TMS and reaches an optimum at 0.2 mL. When 0.2 mL TMS is deposited on the rayon flock synthetic leather surface, the sample will have the highest contact angle value ( $135 \pm 0.1$ ). Due to this high contact angle, the contact area between the water droplet and the rayon flock synthetic leather would be minimized and thus the water droplet can slide easily, leading to a low sliding angle.

### 3.4. Optimum Treatment Parameters

There is a pronounced improvement in the contact angle after TMS plasma treatment. The contact angle of the untreated sample is  $0^\circ$ , whereas that of the plasma modified sample, under the optimum treatment parameters (amount of TMS = 0.2 mL; discharge power = 50 W; flow rate of helium = 12.5 LPM; jet distance = 10mm; and treatment time = 30 s), is  $135^\circ$  (Figure 7 shows an example of contact angle of plasma-modified sample). By definition, a contact angle greater than  $90^\circ$  denotes a hydrophobic surface. Based on the experimental results, under the optimum treatment parameters, the surface of synthetic leather can be made hydrophobic.

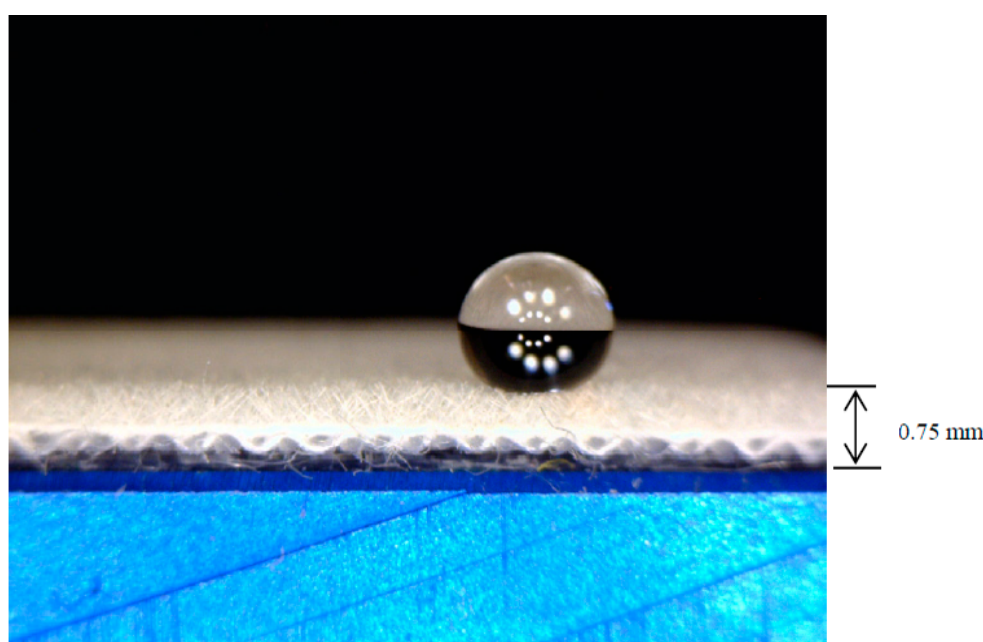


**Figure 7.** Photo showing contact angle of plasma-modified sample.

### 3.5. Surface Energy

Figure 8 shows the change of surface energy in the TMS plasma-modified rayon flock synthetic leather as a function of discharge power. The surface energy of treated samples decreases as the discharge power increases. The surface energy drops dramatically as the discharge power increases from 30 W to 50 W. The reduction of polar surface energy is found to be the most significant at 50 W. A further increase in the discharge power does not affect the surface energy (for example, 60 W). The untreated sample possesses a surface energy of 73.35 mN/m. The surface energy drops to 2.40 mN/m after plasma treatment at a discharge power of 50 W, which is 1/30th of the original value. This result indicates that TMS plasma treatment can effectively lower the surface energy of rayon flock synthetic leather.

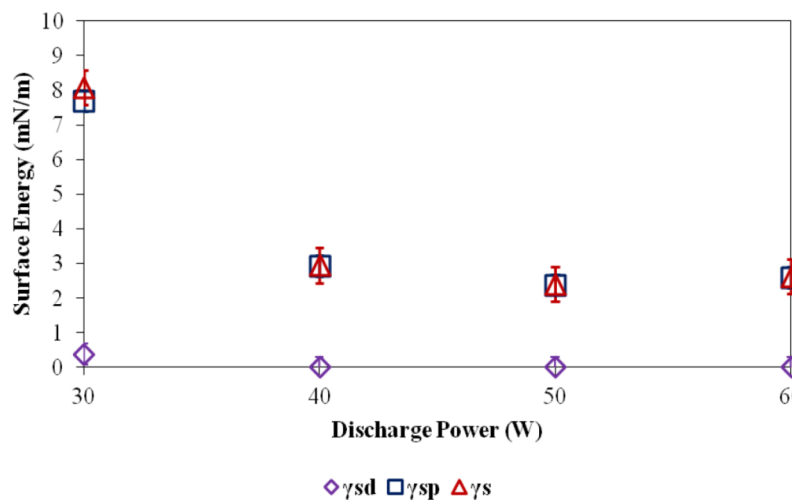


**Figure 8.** The change of surface energy of TMS plasma modified rayon flock synthetic leather (treatment parameter: amount of TMS = 0.2 mL; flow rate of helium = 12.5 LPM; jet distance = 10 mm; treatment time = 30 s).

### 3.6. FTIR-ATR

Figure 9 shows the FTIR spectra of TMS plasma-modified rayon flock synthetic leather with different flow rates of helium. Figure 9a shows the FTIR spectrum of untreated sample while the TMS plasma-modified samples exhibit features of increase in the peak of  $3790\text{ cm}^{-1}$  (OH stretch) and  $1016\text{ cm}^{-1}$  (Si–O–Si antisymmetric stretch), as shown in Figure 9b–e. The FTIR-ATR results confirm the deposition of TMS on sample surface. As the flow discharge increases from 30 W to 50 W, the silicon-related absorbance increases. The greatest intensity of the silicon-related peaks occurs at a discharge power of 50 W, but it drops at 60 W. This indicates that a discharge power of 50 W facilitates the deposition of TMS. In addition, after plasma treatment, the intensity of peaks at  $2900\text{--}3000\text{ cm}^{-1}$  increases significantly, which also indicates that TMS was deposited in the sample surface.

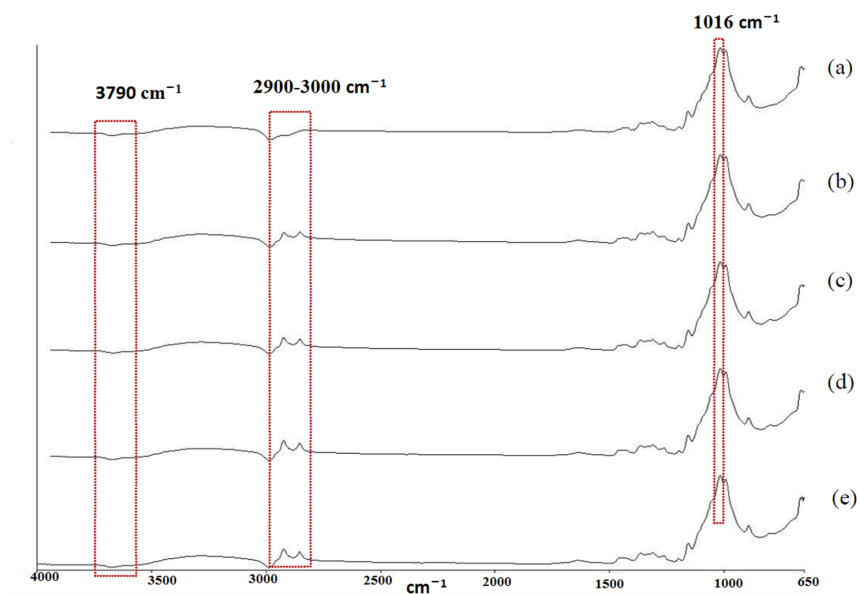


**Figure 9.** FTIR spectra of rayon flock synthetic leather after TMS plasma treatment with different discharge powers: (a) untreated, (b) 30 W, (c) 40 W, (d) 50 W, and (e) 60 W. (Amount of TMS = 0.2 mL; flow rate of helium = 12.5 LPM; jet distance = 10 mm, treatment time = 30 s.)

### 3.7. XPS

XPS analysis is conducted to evaluate the surface chemical composition of TMS plasma modified rayon flock synthetic leather. The surface stoichiometry was analyzed by studying the content of elements of carbon (C), oxygen (O), and silicon (S). Figure 10 shows the wide scan of the untreated and plasma modified, XPS results. The intensity of oxygen sharply decreased after TMS plasma treatment. The spectra features, along with binding energies and full width at half maximum (FWHM) of the treated samples, are reported in Table 4. The carbon and oxygen signals are composed of various peaks indicating the presence of different chemical surroundings of carbon and oxygen atoms. Table 5 shows the peak positions of the C1s features of plasma-modified samples. Deconvolution study reveals that the C1s peak was assigned to be C–H, C–O, O–C–O and C=O bonds (Figure 11). It is clear that the C–O, O–C–O, and C=O bonds' intensity decreased after TMS plasma treatment. The O-containing groups are dropped after TMS plasma treatment. On the contrary, the intensity of C–H bonds increases. H-containing groups, which are generated from TMS during plasma treatment, increase.

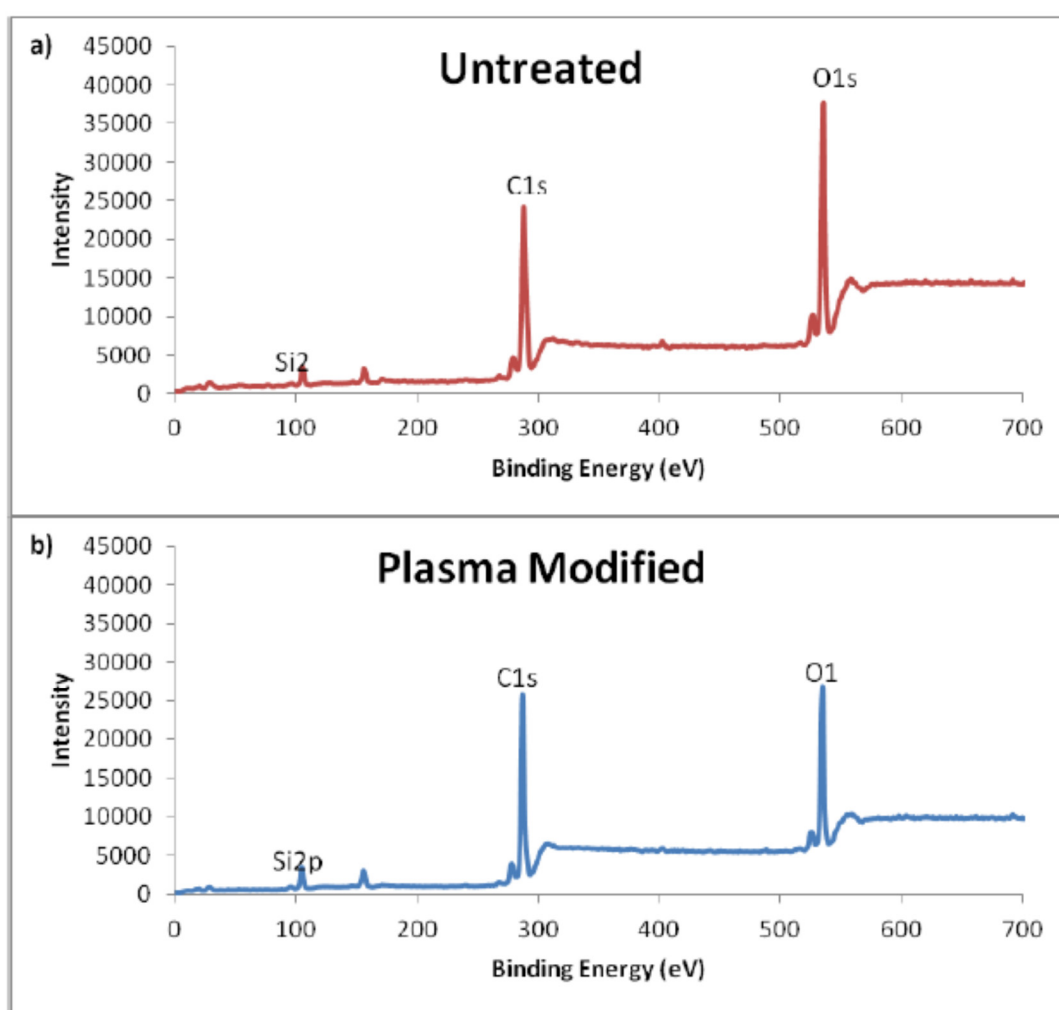


**Figure 10.** Surface elementary composition of (a) untreated and (b) TMS plasma-modified rayon flock synthetic leather (treatment parameters: amount of TMS = 0.2 mL; flow rate of helium = 12.5 LPM; discharge power = 50 W; jet distance = 10mm; treatment time = 30 s).

**Table 4.** XPS features of plasma-modified rayon flock synthetic leather.

Peak	Position (eV)	FWHM
C1s	284.08–292.15	1.01–1.67
O1s	531.50–538.30	1.00–2.03
Si <sub>2p</sub>	102.05–107.39	1.88

**Table 5.** XPS position of C1s features of plasma-modified rayon flock synthetic leather.

Peak	Feature	Peak Position (eV)
C1	C–H, C–C	285.0
C2	C–O	286.9
C3	C=O	288.0
C4	O–C–O	288.7

Chemical deposition is the basic mechanism of TMS plasma treatment. Table 6 shows results for the atomic percentage of rayon flock synthetic leather surface under the influence of different amounts of TMS used in the plasma treatment. Generally speaking, C and Si increase whereas O decreases with the increasing amount of TMS. Except for the case of treating with helium plasma only, the helium plasma provides an etching effect on the leather surface [21], which would reduce the atomic amount of Si. The surface hydrophobicity can be determined by the presence of O-containing groups, which have a strong affinity towards polar wetting agents. The atomic content of O decreases gradually after plasma treatment with increasing amount of TMS (0.1 mL to 0.25 mL) (Table 6). The O/C ratio is an indicator of the surface polarity of a substrate [23–25]. The O/C ratio of untreated and helium plasma-only treated samples have the same O/C ratio. This indicates that they have similar surface polarity and both obtain a 0° contact angle. The O/C ratio of a TMS plasma-modified sample is lower than the original value reported in Table 6, which is gradually decreasing with the increasing amount of TMS. The O/C ratios of 0.2 mL TMS and 0.25 mL TMS are the same, which means that the surface polarity becomes stable and no further change of surface hydrophobicity would occur. Simultaneously, the absence of polar nitrogen (N)-containing groups is another indicator of the increase of surface hydrophobicity. The small amount of N-containing groups in the untreated sample is absent after plasma treatment with TMS. On the other hand, the silicon (Si)-containing groups increase after plasma treatment (Table 6). The Si-containing groups of the plasma-modified sample increase gradually under the influence of increasing amount of TMS when compared with the untreated sample. The Si/O ratio is important for predicting hydrophobicity: the higher the ratio, the more hydrophobic the surface is. Si-containing groups are successfully deposited onto the sample surface by TMS plasma treatment. There is an increase in the Si/O ratio until it reaches a maximum value of 0.2 mL. This result is supported by the SEM results, in which maximum amount of TMS was deposited with the use of 0.2 mL TMS in the plasma treatment. The XPS results (with an increase in the Si/O ratio) can also help to explain the contact angle results, in which the 0.2 mL TMS deposited on the rayon flock synthetic leather surface can greatly improve the contact angle value.

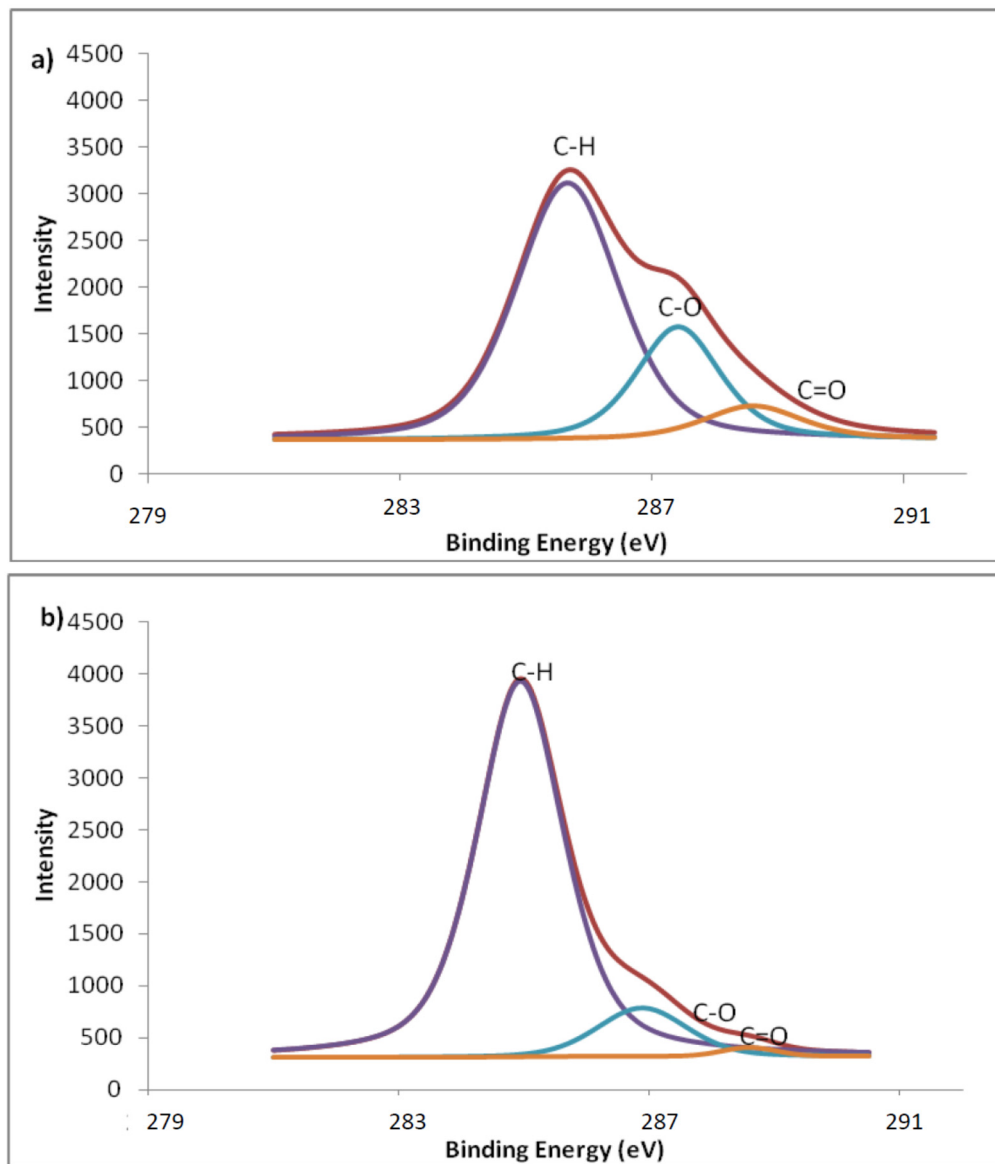


**Figure 11.** XPS deconvoluted C1s peak in (a) untreated sample and (b) plasma-modified rayon flock synthetic leather (treatment parameters: amount of TMS = 0.2 mL; flow rate of helium = 12.5 LPM; discharge power = 50 W; jet distance = 10 mm; treatment time = 30 s).

**Table 6.** Atomic percentage and ratio of rayon flock synthetic leather surface.

Sample	C	O	Si	N	O/C	Si/O
Untreated	61.17	32.02	5.54	1.27	0.52	0.17
0 mL TMS (treated with He plasma only)	62.32	32.52	3.89	1.27	0.52	0.12
0.1 mL TMS	64.37	29.45	6.18	N/A	0.46	0.21
0.15 mL TMS	66.29	27.19	6.52	N/A	0.41	0.24
0.2 mL TMS	66.44	26.08	7.48	N/A	0.39	0.29
0.25 mL TMS	67.01	26.18	6.81	N/A	0.39	0.26

(Treatment parameters: flow rate of helium = 12.5 LPM; discharge power = 50 W; jet distance = 10 mm; treatment time = 30 s)

The XPS results confirm the FTIR-ATR results: Si-containing groups increased after plasma treatment. With the FTIR-ATR and TMS results, the nubs and burrs observed on the surface of plasma-modified samples are proved to be silicon compounds deposited by plasma treatment.

TMS plasma treatment successfully enhances the surface hydrophobicity of rayon flock synthetic leather. The improvement of surface hydrophobicity is attributed to the deposition of organosilicon by plasma treatment [26–28].

### 3.8. Multiple Linear Regression Analysis

In order to examine the effects of plasma process parameters on enhancing surface hydrophobicity and the correlations among the effects of individual parameters, multiple linear regression analysis was employed. The parameters are flow rate of helium, amount of TMS, and discharge power. Multiple linear regression is used as an analyzing tool to investigate the associations between particular independent variables and the dependent variable, even with existence of correlations between independent variables. Multiple linear regression was applied to analyze the effects of the independent variables—discharge power (Power), amount of TMS (TMS), and flow rate of helium (Helium)—on a dependent variable, contact angle (CA), by means of software SPSS. Table 7 indicates that the amount of TMS is highly related to contact angle (within a 95% confidence interval). The amount of TMS applied is critical for enhancing surface hydrophobicity. On the contrary, the flow rate of helium and discharge power were found to have less significant effects. According to Table 8, the adjusted square  $R^2$  is 0.733, which means that 73.3% of the variance in contact angle can be predicted from the independent variables. Sweet and Grace-Martin suggested that the fitness of the regression model is acceptable if the R-square is greater than 0.6.

R-square statistics indicate the model's fitness by representing the percentage of dependent variations that fit into the linear regression model. The significance of the F-test for this regression model is smaller than 0.000; the model is highly able to predict the contact angle with the independent variables with a 95% confidence level.

Table 8 shows a comparison of the contributions of the independent variables by standardized coefficients that convert the variables to the same scale. The regression coefficient of flow rate of helium is  $-0.071$ . The negative result indicates that the contact angle decreases as the flow rate of helium increases. This agrees with the result in the findings that a low flow rate facilitates plasma deposition. On the other hand, the regression coefficients are 0.804 and 0.248 for amount of TMS and discharge power, respectively. The positive sign indicates that the contact angle increases as the discharge power or amount of TMS increases. Having the highest coefficient (0.804) among all independent variables, the amount of TMS contributes strongly to contact angle results. All the relationships are highly statistically significant (significance: 0.000) except flow rate of helium. The flow rate of helium contributes relatively less to plasma deposition. In fact, the flow rate of helium provides a medium for ionization instead of being a critical factor for the deposition.

**Table 7.** Significance of the model parameters.

Independent Variable	Significance (1-Tailed)
Helium	0.334
TMS	0.000
Power	0.298

**Table 8.** Coefficients of the regression model.

Independent Variable	Unstandardized Coefficients	Standardized Coefficients	Collinearity Statistics Tolerance
(Constant)	-69.216	N/A	N/A
Helium	-0.642	-0.071	1.000
TMS	548.704	0.804	1.000
Power	0.846	0.248	1.000

The Collinearity Statistics Tolerance demonstrates the proportion of variation of an independent variable not explained by the linear relationships with other independent variables. A value close to 1 indicates no multicollinearity problem, whereas a value close to 0 indicates a multicollinearity problem. Table 8 shows that the tolerance values of all the independent variables are equal to one. Hence, all independent variables are highly correlated and have stable standard errors for the regression coefficient.

#### 4. Conclusion

High hydrophobicity was imparted to the surface of rayon flock synthetic leather. TMS was used as the precursor for imparting hydrophobicity by plasma treatment. The results show that plasma treatment with TMS enhances surface hydrophobicity. Adequate discharge power (50 W) is required to maintain stable ionization. The flow rate of helium did not contribute much to the resulting hydrophobic alteration. A jet distance of 10 mm is suggested as it allows the short lifetime ions to reach the substrate without degrading the sample surface (due to the heating effect of plasma jet). With the optimum treatment parameters, a highly hydrophobic surface of rayon flock synthetic leather was achieved with a deionized water contact angle of 135° (untreated sample = 0°). SEM, FTIR, and XPS results confirm that silicon compounds were successfully deposited on the sample surface and the reduction of the atomic content of polar O-containing groups. Multiple linear regression analysis confirms the correlations between plasma process parameters. The amount of TMS and discharge power shows significant correlations with the surface hydrophobicity enhancement.

**Acknowledgments:** The authors would like to acknowledge the financial support from Hong Kong Polytechnic University for this work.

**Author Contributions:** C.W.K., C.H.K. and S.P.N. conceived and designed the experiments; C.H.K. performed the experiments and wrote the paper; C.W.K. and S.P.N. provided technical and scientific advice during the experiments; C.W.K., C.H.K. and S.P.N. analyzed the data.

**Conflicts of Interest:** The authors declare no conflict of interest.

#### References

1. Shang, M.H.; Wang, Y.; Limmer, S.J.; Chou, T.P.; Takahashi, K.; Cao, G.Z. Optically transparent superhydrophobic silica-based films. *Thin Solid Films* **2005**, *472*, 37–45. [[CrossRef](#)]
2. Huang, L.; Lau, S.P.; Yang, H.Y.; Leong, E.S.P.; Yu, S.F.; Prawer, S. Stable superhydrophobic surface via carbon nanotubes coated with a ZnO thin film. *J. Phys. Chem. B* **2005**, *109*, 7746–7748. [[CrossRef](#)] [[PubMed](#)]
3. Lee, H.J.; Michielsen, S. Preparation of a superhydrophobic rough surface. *J. Polym. Sci. Part B Polym. Phys.* **2007**, *45*, 253–261. [[CrossRef](#)]
4. Kim, S.H.; Kim, J.; Kang, B.; Uhm, H. Superhydrophobic CF<sub>x</sub> coating via in-line atmospheric RF plasma of He–CF<sub>4</sub>–H<sub>2</sub>. *Langmuir* **2005**, *21*, 12213–12217. [[CrossRef](#)] [[PubMed](#)]
5. Tsougeni, K.; Vourdas, N.; Tserepi, A.; Gogolides, E. Mechanisms of oxygen plasma nanotexturing of organic polymer surface: stable super hydrophilic to super hydrophobic surfaces. *Langmuir* **2009**, *25*, 11748–11759. [[CrossRef](#)] [[PubMed](#)]
6. Raballand, V.; Benedikt, J.; von Keudell, A. Deposition of carbon-free silicon dioxide from pure hexamethyldisiloxane using an atmospheric microplasma jet. *Appl. Phys. Lett.* **2008**, *92*, 091502. [[CrossRef](#)]
7. Kwong, C.H.; Ng, S.P.; Kan, C.W.; Yuen, C.W.M.; Chan, C.K.; Molina, R. Plasma treatment to enhance hydrophobicity of textiles. *Textile Asia* **2013**, *44*, 20–23.
8. Man, W.S.; Kan, C.W.; Ng, S.P.; Yuen, C.W.M.; Chan, C.K. Pigment application on fabric with atmospheric pressure plasma. *Textile Asia* **2013**, *44*, 17–19.
9. Lam, C.F.; Kan, C.W.; Chan, C.K.; Ng, S.P.; Yuen, C.W.M. Plasma treatment in cotton desizing. *Textile Asia* **2013**, *44*, 17–19.
10. Schütze, A.; James, Y.J.; Steven, E.B.; Park, J.; Selwyn, G.S.; Hicks, R.F. The atmospheric-pressure plasma jet: A review and comparison to other plasma sources. *IEEE Trans. Plasma Sci.* **1998**, *26*, 1685–1694. [[CrossRef](#)]
11. Cheng, C.; Liye, Z.; Zhan, R.J. Surface modification of polymer fibre by the new atmospheric pressure cold plasma jet. *Surf. Coat. Technol.* **2005**, *200*, 6659–6665. [[CrossRef](#)]

12. Fonseca, J.L.C.; Apperley, D.C.; Badyal, J.P.S. Plasma polymerization of tetramethylsilane. *Chem. Mater.* **1993**, *5*, 1676–1682. [[CrossRef](#)]
13. Favia, P.; Lamendola, R.; D'Agostino, R. The role of substrate temperature and bias in the plasma deposition from tetramethylsilane. *Plasma Sources Sci. Technol.* **1992**, *1*, 59–66. [[CrossRef](#)]
14. Fonseca, J.L.C.; Tasker, S.; Apperley, D.C.; Badyal, J.P.S. Plasma-enhanced chemical vapor deposition of organosilicon materials: A comparison of hexamethyldisilane and tetramethylsilane precursors. *Macromolecules* **1996**, *29*, 1705–1710. [[CrossRef](#)]
15. Park, S.Y.; Kim, H.; Hong, S.U.; Sasabe, H. Plasma polymerization of hexamethyldisilazane. *Polym. J.* **1990**, *22*, 242–249. [[CrossRef](#)]
16. Kan, C.W.; Kwong, C.H.; Ng, S.P. Hydrophobisation of hydrophilic imitation leather with polyester surface by atmospheric pressure plasma treatment. *J. Textile Inst.* **2016**, *107*, 91–94. [[CrossRef](#)]
17. Kan, C.W.; Kwong, C.H.; Ng, S.P. Surface Modification of polyester synthetic leather with tetramethylsilane by atmospheric pressure plasma. *Appl. Surf. Sci.* **2015**, *346*, 270–277. [[CrossRef](#)]
18. Kan, C.W.; Kwong, C.H.; Ng, S.P. Effect of plasma treatment on the hydrophobicity of imitation leather with 100% polyurethane surface. *Fibers Polym.* **2015**, *16*, 702–704. [[CrossRef](#)]
19. Kwong, C.H.; Ng, S.P.; Kan, C.W.; Molina, R. Inducing hydrophobic surface on polyurethane synthetic leather by atmospheric pressure plasma. *Fibers Polym.* **2014**, *15*, 1596–1600. [[CrossRef](#)]
20. Kan, C.W.; Kwong, C.H.; Ng, S.P.; Yuen, C.W.M. Treating of rayon-flocked fabric by atmospheric pressure plasma. *Mater. Sci. Medzg.* accepted.
21. Kan, C.W.; Yuen, C.W.M. Effect of atmospheric pressure plasma treatment on wettability and dryability of synthetic textile fibres. *Surf. Coat. Technol.* **2013**, *228*, S607–S610. [[CrossRef](#)]
22. Kaelble, D.H. Dispersion-polar surface tension properties of organic solids. *J. Adhes.* **1970**, *2*, 66–81. [[CrossRef](#)]
23. Gao, Q.; Zhu, Q.; Guo, Y.; Yang, C.Q. Formation of highly hydrophobic surface on cotton and polyester fabrics using silica sol nanoparticles and nonfluorinated alkylsilane. *Ind. Eng. Chem. Res.* **2009**, *48*, 9797–9803. [[CrossRef](#)]
24. Paynter, R.W. XPS studies of the ageing of plasma-treated polymer surfaces. *Surf. Interface Anal.* **2000**, *29*, 56–64. [[CrossRef](#)]
25. Tsoi, W.Y.I.; Kan, C.W.; Yuen, C.W.M. Using ageing effect for hydrophobic modification of cotton fabric with atmospheric pressure plasma. *BioResources* **2011**, *6*, 3424–3439.
26. Inagaki, N.; Katsuoka, H. Gas separation membranes made by plasma polymerization of silanes and fluoromethane. *J. Membr. Sci.* **1987**, *34*, 297–305.
27. Tajama, I.; Yamamoto, M. Characterization of plasma polymers from tetramethylsilane, octamethylcyclotetrasiloxane, and methyltrimethoxysilane. *Polym. Sci. Part A Polym. Chem.* **1987**, *25*, 1737–1744. [[CrossRef](#)]
28. Coopes, I.H.; Griesser, H.J. The structure of organosilicon plasma-polymerized coatings on metal substrates. *J. Appl. Polym. Sci.* **1989**, *37*, 3413–3422. [[CrossRef](#)]

